EARTH SURFACE PROCESSES AND LANDFORMS
Earth Surf. Process. Landforms **39**, 438–449 (2014)

Published online 6 August 2013 in Wiley Online Library
(wileyonlinelibrary.com) DOI: 10.1002/esp.3456

Two-dimensional modelling of large wood transport during flash floods

Virginia Ruiz Villanueva,[1]* Ernest Bladé Castellet,[2] Andrés Díez-Herrero,[1] José M. Bodoque[3] and Martí Sánchez-Juny[2]
[1] Department of Research and Geoscientific Prospective, Geological Survey of Spain, Madrid, Spain
[2] Department of Hydraulic, Maritime and Environmental, Flumen Institute, Technical University of Catalonia (UPC), Barcelona, Spain
[3] Castilla La Mancha University, Mining and Geological Engineering, Toledo, Toledo, Spain

Received 6 December 2012; Revised 4 June 2013; Accepted 10 June 2013

*Correspondence to: Virginia Ruiz-Villanueva, Department of Research and Geoscientific Prospective, Geological Survey of Spain, Rios Rosas 23, Madrid, ES 28003, Spain. E-mail: virginiaruizv@gmail.com

ESPL
Earth Surface Processes and Landforms

ABSTRACT: Large woody material (LWM) transported by rivers may be entrapped at critical stream geometry configurations (e.g. bridges) and therefore dramatically increase the destructive power of floods. This was the case in a Spanish mountain river where a flood event with a high degree of LWM transport took place in 1997. The aim of this study was to simulate a bridge clogging process and reconstruct the wood deposit patterns, modelling individual pieces of wood moving with the water flow and interacting among them and with the bridge. A two-dimensional numerical model was developed to simulate the transport of LWM and its effect on hydrodynamics. Different scenarios for the wood transport rate allowed us to study the influence of inlet boundary conditions on bridge clogging. For the studied event, the scenario which best reproduced the bridge clogging effect and flood characteristics was one in which 60% of the total wood entered before the peak discharge. This dropped to 30% at the peak itself, and finally fell to 10% during the recession curve. In addition, the accumulation patterns of LWM along the reach were computed and compared with post-event field photographs, showing that the model succeeded in predicting the deposition patterns of wood and those areas prone to form wood jams. Copyright © 2013 John Wiley & Sons, Ltd.

KEYWORDS: large woody material; Iber 2D model; bridge clogging; hydrodynamics; woody debris

Introduction

Large woody material (LWM) plays an important role in river ecosystems by influencing hydrology, hydraulics, sedimentology, and morphology (Lassettre and Harris, 2001; Gurnell *et al.*, 2002; Montgomery, 2003; Seo *et al.*, 2008). In addition, an extensive literature now exists describing the influence of wood on stream ecology (Gippel and White, 2000; Martin and Benda, 2001; Gregory *et al.*, 2003), since wood may provide a habitat for fish and riverine species (Carlson *et al.*, 1990; Jackson and Sturm, 2002; Langford *et al.*, 2012, and references cited therein) and regulates water flows and nutrient fluxes (Welty *et al.*, 2002).

Recent research has focused on the mobilization of woody material during floods, since transported woody material can represent a substantial increase in the destructive power of floods (Diehl, 1997; Fischer, 2006; Lyn *et al.*, 2007; Waldner *et al.*, 2007; Comiti *et al.*, 2008; Mao *et al.*, 2008; Mazzorana *et al.*, 2009; Comiti *et al.*, 2012). LWM may reduce the capacity of bridge openings, contribute to scour, and increase lateral forces on bridges. The main results of these phenomena are a quick succession of backwater effects with bed aggradation, flow diversions and local scouring processes, ultimately evolving towards embankment/bridge collapse and floodplain inundations. As a result, flooded areas may be different from those predicted in the absence of wood (Ruiz-Villanueva *et al.*, 2012a).

In this context, it has been demonstrated that wood removal could fail, in part because of new inputs of wood (Young, 1991; Gippel, 1995; Dudley *et al.*, 1998). For this reason, the problem has been redefined as the inability of infrastructures to allow LWM to pass (Lassettre and Kondolf, 2012).

In forested mountain catchments, most trees fall into the stream as a result of a variety of mechanisms such as mass wasting, channel migration and bank undercutting (May and Gresswell, 2003; Swanson, 2003), windthrow and fire (Benda and Sias, 2003; Rosso *et al.*, 2007) or natural tree mortality (Benda *et al.*, 2003). During floods, the number of wood pieces likely to be transported may increase significantly (Nakamura *et al.*, 2000). A better understanding of LWM entrainment, or the process by which woody material is transported to the river, is therefore needed (May and Gresswell, 2003; Bragg and Kershner, 2004; Mazzorana *et al.*, 2009; Rigon *et al.*, 2012; Ruiz-Villanueva *et al.*, 2012b).

There are few direct observations and/or measurements of the conditions of wood entrainment and transport during floods (see pioneering studies in MacVicar *et al.*, 2009). Physical models and flume experiments have been used to overcome these constraints, contributing greatly to our present knowledge of LWM transport (Braudrick and Grant, 2000; Braudrick *et al.*, 2001; Bocchiola *et al.*, 2002; Haga, 2002; Schmocker and Hager, 2011). Some others have used one-dimensional (1D)

or two-dimensional (2D) models (Mazzorana *et al.*, 2010; Merten *et al.*, 2010; Comiti *et al.*, 2012), by first computing the hydraulics (in 1D or 2D) and then using the results to calculate wood mobilization.

However, there have been no deterministic models for predicting wood transport volume at relatively short timescales to date. Recently, a 2D numerical model was developed and proposed by Ruiz-Villanueva (2012) and Ruiz-Villanueva *et al.* (submitted for publication) to simulate LWM transport together with hydrodynamics. This model was added as a new module (*Woody Iber*) into the existing Iber model, a 2D hydrodynamic software application (www.iberaula.es; Corestein *et al.*, 2010; Bladé *et al.*, 2012a; Bladé *et al.*, 2012b) based on the finite volume method. The new module was developed to compute log motion, which considers a threshold water velocity and a description of log motion based on the force balance. Water flow variables affected by the influence of log presence are computed using a 2D hydrodynamic model enhanced with drag terms produced by log resistance to the flow. Flume experiments were used to test and validate the correct performance of the numerical model. The good agreement observed between the numerical model and prototype-scale simulations of log transport substantiates the validity of the proposed approach, although notable simplifications were adopted for development of the presented tool, such as cylinders being used as log shapes. Therefore, one of the aims of this study is to test the proper operation of the new module and its ability to provide a suitable model for a natural watercourse. A further aim is to simulate a bridge clogging process during a flash flood caused by LWM transport by modelling individual wood pieces in the simulation. The interaction between the logs and the bridge is then simulated and the effect on hydrodynamics analysed. Wood deposit patterns are also examined.

The area selected for the study is a mountain catchment where a flood event with a high degree of LWM transport took place in 1997 and where the necessary data are available.

Study Area and 1997 Flash Flood Description

The study area is located in southwest Europe, in the central part of the Iberian Peninsula. The study site is a short reach of the Arroyo Cabrera stream, a tributary of the Alberche River in the Tagus River Basin, on the northern slopes of the Sierra de Gredos, in the Spanish Central System (Figure 1). This small poor-gauged forested mountain catchment covers an area of over 15·5 km^2 and the altitude range is 1168 m [maximum elevation 1923 and minimum 755 m above sea level (a.s.l.)]. The main channel is 5500 m long, with an average slope of 21.6%. Table I shows the main characteristics of the basin and the studied reach.

The geology consists mainly of Upper Palaeozoic granitoids covered by superficial Quaternary formations of conglomerates, gravels, sands and silts.

The local forest stand is formed predominantly by *Pinus pinaster*, *Pinus sylvestris* and *Quercus pyrenaica*. In addition, riparian broadleaved species *Alnus glutinosa* and *Fraxinus angustifolia* can be found on both river banks.

The continental Mediterranean climate of the study area is typical of Spanish medium mountain ranges. The mean annual temperature is 14·6 °C with 554 mm mean annual rainfall in the lower part and up to 2000 mm on the higher land (Palacios *et al.*, 2010).

Torrential rainfall events usually occur in autumn and winter, resulting in abundant surface runoff, sediment mobilization and related flash-flood events. The most important event identified to date was the 1997 flash flood. The chronological description of the 1997 process can be summed up as follows: a shallow landslide triggered in the upper part of the catchment evolved into a hyper-concentrated flow (Bodoque *et al.*, 2011; Ruiz-Villanueva *et al.*, 2011). At 3·2 km downslope most of the sediment transport was partially deposited and an avulsion took place. This process led to a major change in the drainage network

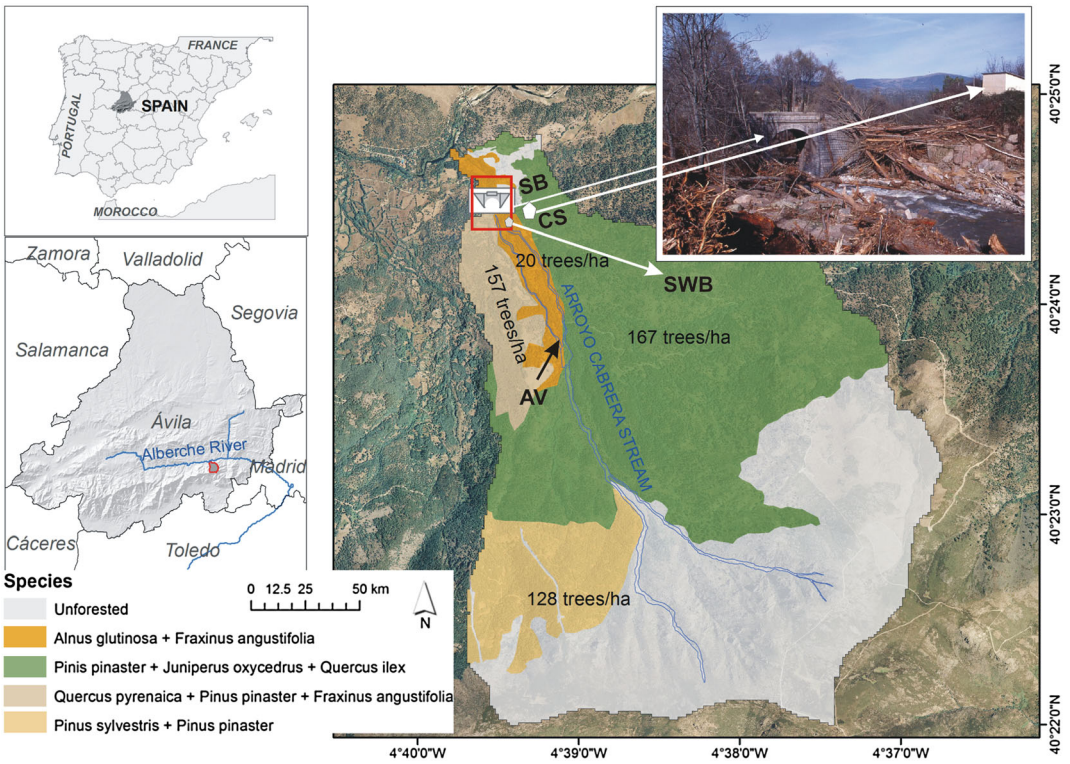

Figure 1. Location of the study area (red rectangle): Arroyo Cabrera stream basin with vegetation density and species, and location and picture of the bridge affected by wood clogging (SB); camping site located in the riverside (CS); the small white building with a high water mark of the 1997 flood (SWB); and the avulsion (AV). This figure is available in colour online at wileyonlinelibrary.com/journal/espl

Table I. Main physical characteristics of the Arroyo Cabrera catchment and the studied reach

	Values	Unit
Drainage area	15·5	km^2
Minimum basin elevation	755	m a.s.l.
Maximum basin elevation	1923	m a.s.l.
Length of the main channel	5·5	km
Mean gradient of the main channel	21	%
Stream order	3	—
Basin time of concentration	1·5	h
Mean annual precipitation (lowland)	554	mm
Mean annual precipitation (high altitude)	~2000	mm
Maximum water discharge recorded[a]	45·6	$m^3\ s^{-1}$
Length of the studied reach	250	m
Maximum studied reach elevation	805	m a.s.l.
Minimum studied reach elevation	755	m a.s.l.
Studied reach bed slope	0·034	—

[a]The value refers to the flow gauge installed since 2004.

pattern, and remobilized large quantities of sediment, damaging the vegetation located within the stream and on the banks and resulting in a substantial wood recruitment process.

Upstream from the point where the Arroyo Cabrera flows into the Alberche River there is a critical section in the outlet of the catchment; there is a bridge which is the biggest obstacle in the stream and where large deposits of wood and boulders were observed after the 1997 flash flood event (Figure 1).

Upstream from the avulsion point (AV in Figure 1) wood jams or individual pieces of wood deposited were not observed in the channel or on the riverside, although several toppled trees were seen lying transversal or oblique to the flow direction, together with many uprooted tree stumps. Along this reach, the main recruitment was from processes on the upper slopes and the destabilizing action from the knock-on effect of the bedload transport.

Three small blocks and boulders lobes were deposited upstream of this avulsion point. The secondary channel developed downstream with a maximum width of 35 m and extended 1 km before flowing into the main channel again.

In the small white building (SWB in Figure 1) and surroundings evidence of the water depth could clearly be identified. The silt deposit on the building (as a high water mark, HWM), and the damaged trees showing scars [as palaeostage indicators (PSIs); Ballesteros *et al.*, 2011a; Ballesteros *et al.*, 2011b] were used to reconstruct the water depth. Finally, the largest obstacle in the stream, the studied bridge (SB in Figure 1), is where important deposits of wood and boulders were observed.

Methodology

The procedure applied to the 1997 event study is divided into three main stages (Figure 2): (1) estimation of the large wood recruited at a basin scale (analysing the recruitment areas caused by avulsion, fluvial transport and bank erosion occurred during the 1997 event); (2) establishment of the inlet boundary conditions at the studied reach (water and wood fluxes) by means of scenarios; (3) and finally, the modelling of the 1997 flood (including large wood transport).

Therefore, the sections later describe the following stages: (i) gives a brief description of the model developed for simulating wood transport in rivers; (ii) provides a detailed description of methods for simulating the interaction between wood and critical sections such as bridges (weirs and gates); (iii) the inlet boundary conditions (water discharge and wood transport rate) for the studied flood event are estimated and explained; (iv) results validation is described.

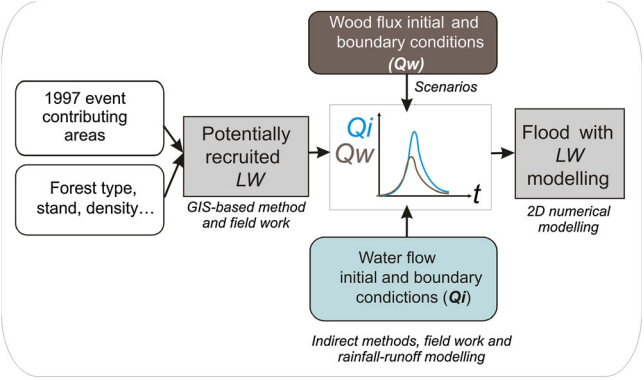

Figure 2. Proposed methodology sketch. Qi and Qw are the inlet flow discharge and inlet wood transport rate, respectively. This figure is available in colour online at wileyonlinelibrary.com/journal/espl

Modelling large wood transport

The transport of wood along the stream during the 1997 event was simulated using a recently developed module for this purpose implemented in a 2D hydraulic model (Iber). The model is described in detail in Ruiz-Villanueva (2012) and Ruiz-Villanueva *et al.* (submitted for publication) and only a brief description was therefore provided in the Introduction section and is completed here.

To solve the hydrodynamics, the Iber model uses the finite volume method with a second order Roe Scheme. This method is especially suitable for flows in mountain rivers, where shocks and discontinuities can occur and flow hydrographs are very sharp. The method is conservative, even when wetting and drying processes take place.

The new module considers wood entrainment and incipient motion performing a balance of the forces acting on each single piece of wood: the gravitational force acting on the log, equal to the effective weight of the log in a downstream direction; the friction force in the opposite flow direction, which is equal to the normal force acting on the log times the coefficient of friction between the wood and the bed; and the drag force, also acting in the flow direction, which is the downstream drag exerted on the log by the water in motion.

The combination of these three forces yields the force balance at incipient motion for a circular cylinder lying on the river bed: $F_f = F_g + F_d$

$$\begin{aligned}&(g\cdot\rho_w\cdot L_w\cdot A_w - g\cdot\rho\cdot L_w\cdot A_{sub})\cdot(\mu_{bed}\cdot\cos\alpha - \sin\alpha)\\&= {U_{flow}}^2/2\cdot\rho\cdot C_d\cdot(L_w\cdot h\cdot\sin\theta + A_{sub}\cdot\cos\theta)\end{aligned} \quad (1)$$

where h is the water depth. Thus, the velocity corresponding to $(F_g + F_d)/F_f = 1$, here called threshold velocity $U_{\lim}$

$$U_{\lim}^2 = \frac{((g\cdot\rho_w\cdot L_w\cdot A_w) - (g\cdot\rho\cdot A_{sub}\cdot L_w)\cdot(\mu_{bed}\cdot\cos\alpha - \sin\alpha))}{(0.5\cdot C_d\cdot\rho\cdot(L_w\cdot h\cdot\sin\theta + A_{sub}\cdot\cos\theta))} \quad (2)$$

The velocity along the transport trajectory for each moving woody material ($U_{\log}$) model log is estimated as

$$U_{\log} = (1 - C^*)\cdot U_{flow} \quad (3)$$

where

$$C^* = U_{\lim}/U_{flow} \quad (4)$$

The movement of wood logs includes two possible transport regimes (floating or sliding) based on wood density, and both translation and rotation, due to the fact that one end of the

piece of wood is moving faster than the other end (based on flow velocity field) and causes the piece to rotate towards a more flow-parallel orientation. The flow velocity at each end (1 or 2) of the log $\mathbf{v}^{1,2} = (v_1, v_2)^{1,2}$ is calculated from the flow velocity at the log centre $\mathbf{v}$, the flow velocity gradients and the relative position of the log ends $\mathbf{x}^{1,2} = \left(x_1^{1,2}, x_2^{1,2}\right)$ with respect to the log centre position $\mathbf{x}$:

$$v_i^{1,2} = v_i + \frac{\partial v_i}{\partial x_j} \cdot \left(x_j^{1,2} - x_j\right) \tag{5}$$

Interactions between logs and the channel configuration and among logs themselves are also taken into account in the model. Therefore, log velocity and trajectory may change due to contact with the banks or with other logs. If one moving piece of wood meets another piece (floating or resting), the two may collide and continue moving at a different velocity (Figure 1). This new velocity or final velocity $(\mathbf{v'}_{\log})^i$ of log i is calculated from the initial velocities $(\mathbf{v}_{\log})^{i,j}$ for both colliding pieces i, j as

$$\left(\mathbf{v'}_{\log}\right)^i = (1+e)\cdot\left(\mathbf{v}_{\log}\right)^{cm} - e\cdot\left(\mathbf{v}_{\log}\right)^i \tag{6}$$

where

$$\left(\mathbf{v}_{\log}\right)^{cm} = \frac{m_i\cdot\left(\mathbf{v}_{\log}\right)^i + m_j\cdot\left(\mathbf{v}_{\log}\right)^j}{m_i + m_j} \tag{7}$$

is the velocity of the mass centre of the colliding logs, e is the restitution coefficient (equal to one assuming elastic interaction) and m_i and m_j are the log masses.

Moreover, when a piece of wood reaches the bank, it can be entrapped and the driving forces decrease due to reduction of the submerged area, but the resisting forces are still active around the log and therefore the initial motion condition is recalculated.

The wood jam formation is a three-dimensional (3D) process; however, this 2D model attempts to reproduce a quasi-3D process. If a log is lying (resting) on the river bed or bank and another piece floats above it, these two may interact, depending on the water depth and log diameters, and the lying log may start to move or the floating log may stop according to the force balance.

The hydrodynamics and wood transport are computed in two related ways; thus, the hydrodynamics influence the wood transport, but the presence of wood also influences the hydrodynamics. A drag force is included in the flow model as an additional term in the Saint Venant equations, similar to roughness. This force is included as an additional shear stress at every finite volume, resulting from the presence of logs.

$$\boldsymbol{\tau}_{wood,i} = \frac{\sum_{\text{logs}} F_d}{A_i} \tag{8}$$

where: $\boldsymbol{\tau}_{wood,i}$ is the shear stress at every finite volume, or mesh element, I; F_d the drag forces; and A_i the volume of the 2D finite volume, or area of mesh element i, that is:

$$\boldsymbol{\tau}_{wood,i} = \left[\sum_{\text{logs}} \left(U - U_{\log}\right)^2 / 2\cdot\rho\cdot C_d\cdot\left(L_w\cdot y\cdot\sin\theta + A_{sub}\cdot\cos\theta\right)\right] / A_i \tag{9}$$

where U is the water velocity; $U_{\log}$ is the component of the log velocity in the direction of the flow; and C_d is the drag coefficient of the wood in water. This last parameter has been analysed extensively before (Manga and Kirchner, 2000). Brooks *et al.* (2006) proposed 1·2 for wood in real streams; and Bocchiola *et al.* (2006) found a value of 1·41 for dowels in flume experiments. In this study, the parameter is assumed to be constant (1·2) but the method allows its value to be changed in each simulation.

Wood and critical stream configurations: internal conditions

Hydraulic structures like gates, weirs or bridges, which change the conditions of the system and therefore cannot be represented by the Saint Venant equations, are usually treated as internal conditions in 2D models. The internal conditions available in the Iber model (similar to most 2D hydraulic models) are: (i) flow below a gate; (ii) flow over a weir; (iii) a weir-gate combination; and (iv) a local loss determined by a loss coefficient. In the case of gates, the standard equation of the flow under a gate, which can be free or submerged, is used. The data to enter are the discharge coefficient, the gate's bottom elevation, the gate opening height and its width. To simulate weirs, the rectangular weir discharge equation for free and submerged flow is used. The data to input are the weir's crest elevation, the discharge coefficient and the weir's length. In this study, the condition used to represent the bridge is a combination of the two previous ones: flow under a gate and over a weir, so all the earlier-mentioned parameters must be used. The total discharge is calculated as the addition of the flow below the gate and the flow above the weir.

A log can pass under or above the bridge deck, or become trapped by the structure, depending on the gate opening and width, or the weir length, water depth and wood diameter (Figure 3). If the water depth (h_1) and wood diameter are greater than the height of the gate (Zg) or less than the height of the weir (Zw), then the wood log will collide with the obstacle; in our case, the deck of the bridge. In this case, from the point of view of wood transport the obstacle is treated as a material wall, and logs interacting with it will bounce back and become trapped. The drag force on trapped logs represents an opposite action to water flow, producing a rise in water depths and a decrease in velocity.

Inlet boundary conditions and scenarios

The inlet water discharge was computed using the available reconstructed flood hydrograph obtained by hydrological simulation in a previous study (Ruiz-Villanueva *et al.*, 2012a),

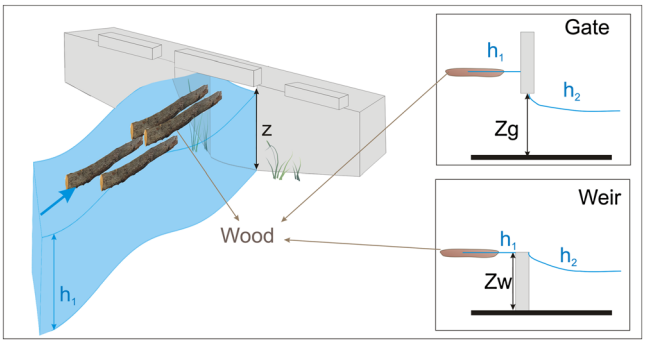

Figure 3. Sketch of the gate and weir internal contour conditions and wood. This figure is available in colour online at wileyonlinelibrary.com/journal/espl

as described previously. The inlet wood boundary conditions were assigned to the whole domain using the affected area and the information available on the forest stand (The Forest Map of Spain and National Forest Inventory produced by the Ministry of the Environment, Spain; MFE, 2011). It was possible to estimate potentially recruited wood volumes (in terms of number of trees; Vw) following the methodology proposed by Ruiz-Villanueva *et al*. (2012b). This method allowed us to estimate the potential amount of wood transported in this event, although some simplification has to be assumed. Data are provided for the three main species in any given area and the total canopy cover (C_i) is a percentage of the total area covered by forest. The inventory contains estimates of tree density (expressed as number of trees per area) for each species for the whole forested territory. This latter density is called relative density per species (D_i) here and is used together with species occupation and canopy cover to estimate the final number of trees in a given area. The value of A_i is the contributing area defined for a specific recruitment process (in this case the area affected by the 1997 flash flood and avulsion):

$$Vw_i = A_i \cdot C_i \cdot D_i \tag{9}$$

In the delineated source area, the probability of a tree entering the stream may vary (Robison and Beschta, 1990). This variability was incorporated into the method using a volume correction factor (Fc), which takes into account vegetation resistance and the severity of the recruitment mechanism. This is equivalent to a recruitment probability and can be 1, 0·5 or 0·1; here it was computed by means of fuzzy logic matrices (see Ruiz-Villanueva *et al*., 2012b, for details). This factor therefore reduces the total number of trees of recruitable wood in those areas where the severity of the process is lowest and/or vegetation resistance highest.

$$Vw_t = Vw_i \cdot Fc \tag{10}$$

Once the number of recruited trees is assessed the number of logs can be estimated, taking into consideration the occurrence of breakage through a coefficient:

$$Logs = k. \cdot Vw_t$$

where k is a coefficient.

According to field observations and photographs, most of the trees were almost whole trees. We estimated the number of trees and logs using $k = 1$. However, uncertainty exists regarding this rule.

Based on knowledge of the riparian vegetation, ranges were established for the diameters, density and lengths of wood. The stochastic variation of these parameters, together with position and initial angle with respect to flow, were then used to characterize each piece of wood entering the simulation.

A series of scenarios were then simulated assuming that the peak in wood transport occurred prior to the peak discharge, and varying the temporal distribution of the wood volume (in terms of number of logs). Therefore, the proposed scenarios are (Figure 4):

- Scenario 1 (congested transport): 100% of total recruited wood enters just before and during the peak discharge and wood transport occurs from the rising limb and during the peak (~1 h).
- Scenario 2 (semi-congested transport): 60% enters before the peak discharge (~0·5 h), during the peak this amount is reduced to 30% (~0·5 h), and finally during the recession curve 10% of the total recruited wood is transported (~0·5 h).

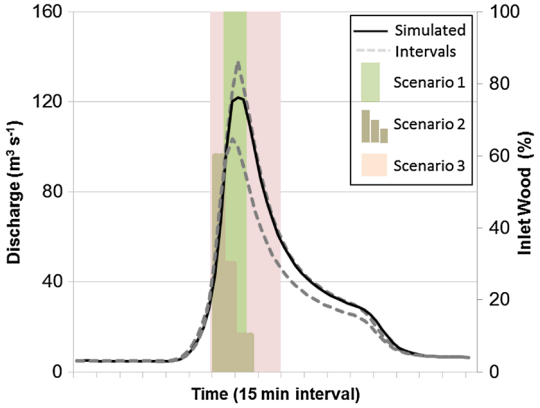

Figure 4. Reconstructed event hydrograph and wood transport scenarios. This figure is available in colour online at wileyonlinelibrary.com/journal/espl

- Scenario 3 (steady transport): the total of recruited trees enter continuously during the whole event until the middle of the recession curve (~3 h).

Since no information was available for establishing initial wood conditions, no log was placed in the reach during the initial time interval.

Results validation

A semi-quantitative validation of the model's results was based on available information and previous works (Díez-Herrero, 2003, and unpublished data; Ruiz-Villanueva *et al*., 2012a), photographs and fieldwork. The evidence from these observations, images and other indicators (e.g. fine sand and coarse wood deposits found on the bridge deck) show that the bridge was flooded due to the clogged wood. In addition, indirect methods (slope conveyance and competence flow equation) together with hydraulic simulation (using 1D Hec-Ras) and rainfall-runoff modelling (using Hec-HMS) were applied to reconstruct the main flash flood parameters at the bridge section and upstream reach. Peak discharge (123 ± 18 m^3 s^{-1}), simulated hydrograph, water depth (~7 m at the bridge section), blockage ratio (48 ± 8% of the bridge section), flow velocity (reach mean 2·85 m s^{-1}), and the flood return period (35 ± 10 years) were estimated for this event (for details see Ruiz-Villanueva *et al*., 2012a).

This information allowed us to set the scenario which best reproduces the 1997 event and analyse the linear patterns of predicted wood deposits. To carry out this spatial patterns evaluation, we used kernel density estimation (KDE). This was computed for the combination of all three scenarios and along both the right and left banks, as well as for defined cross-sections. This non-parametric function evaluates the number of deposited logs within a series of distances centred at each point within the stream reach. We used this estimator to infer the depositional probability and the areas prone to form wood jams, according to the total number of deposited logs.

In addition, the effect of wood transport and deposition on hydrodynamics is analysed. The roughness coefficient was calibrated using the rating curve obtained for the bridge cross-section where a stream gauge has been in place since 2004.

Simulation Results and Validation

After analyzing the affected areas defined for this event, the vegetation resistance and the forest density (three main species,

canopy cover and relative density), theoretical predictions were obtained for the number of trees recruited (Vw) by the flood event.

These estimates and log characteristics (based on National Forest Map and Inventory) are summarized in Table II.

The estimated amount of recruited wood was 186 ± 46 logs. This amount was distributed in time according to the three transport scenarios.

The model's results predict the location of wood deposits and bridge clogging for the three scenarios (Figure 5). As Figure 5 shows, the main depositional areas or areas prone to form wood jams are the two bridge abutments (section D, SB in Figure 5), and along the left bank of the stream, particularly the area between sections A and D, and right bank in the area between sections B and D for SC1 and SC2. Since the characteristics of the logs (length, diameter, initial angle) are randomly selected (between the established ranges), the final logs forming the deposits may vary for each simulation; however, the depositional areas are approximately the same since they are mainly defined by the topography and hydrodynamics and not only the shape of the logs.

Therefore, the mean probability of a log being deposited in a specific place is represented in terms of KDE in Figure 6 for the combination of the three scenarios. This probability may be equivalent to the probability of woody jam formation for both the left and right banks.

This density distribution estimator can also be used to estimate the probability of a log becoming entrapped in the bridge cross-section (Figure 7). This KDE for bridge clogging is up to 30% in SC1, 25% for SC2 and 20% for SC3.

The characteristics of simulated logs were analysed in order to identify different behaviours (Figure 8) between transported and deposited logs.

Table II. Characteristics of the estimated inlet wood

	Mean	Maximum	Minimum
Vw (number of logs)	186	232	140
Length (m)	7	15	2
Diameter (m)	1	1·5	0·5
Wood density (kg m^{-3})	700	800	500

The angle was also analysed with respect to the flow of the simulated logs and observations revealed that the orientation of the transported wood was predominantly parallel (170º to 200º) to the flow but oblique to perpendicular for the deposited wood in general.

As Figure 8 shows, the mean length of the transported logs is 6·65 m and the mean diameter 0·9 m, whereas for deposited logs these values increase up to 9·34 m and 1·1 m, respectively. As expected, the deposited pieces were larger. This distribution is similar for the three scenarios.

In addition, Figures 9–11 show the main characteristics (water depth, flow velocity and flow competence) of the flash flood event for the four scenarios (without wood, and the three scenarios with wood transport).

The water depth for the simulated hydrograph without wood is around 4·7 m at the bridge section; this value is in the same range as that obtained in the previous study, which was around 4·5 m. Although the backwater effect due to bridge clogging increases this level up to 7·1 m according to previous work, 7·3 m was the result obtained in Scenario 2 of this reconstruction. In Scenario 1, this level could increase to more than 8 m (1 m above the bridge deck). Scenario 3 is an intermediate case, where the bridge is less blocked and the water depth does not reach the bridge deck, rising only to 6·8 m.

The other HWM used for the reconstruction was located in the small white building situated on the right bank. This mark was 2·9 m. Scenario 1 shows a water depth of above 3 m, Scenario 2 gives a value of 2·8 m and Scenario 3 one of 2·3 m.

The main velocity estimated for this event was around 3·5 m s^{-1} before the bridge obstruction. Although these values are exceeded locally, the main flow velocity agrees with these previous estimates. In addition, as the bridge is increasingly obstructed, it can be observed how the flow velocity decreases upstream.

Table III summarizes these values as well as the final number of logs deposited and the blockage percentage of the bridge.

The main effect of bridge clogging due to wood transport on flow competence is a decrease in this parameter (Figure 11) due to the decrease in flow velocity. While the left bank is where most of the wood is deposited, on the right bank bigger boulders are observed in the post-event pictures, as well as erosive marks.

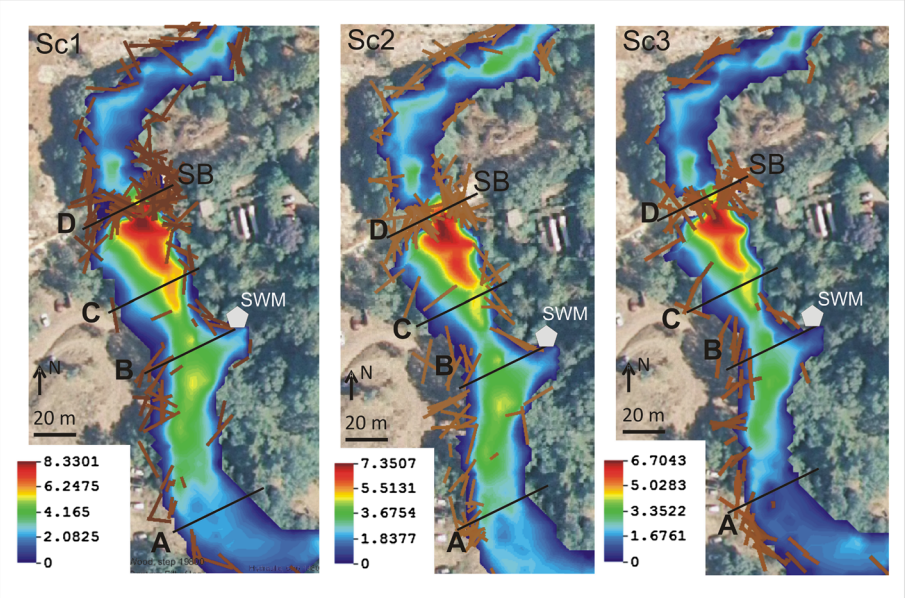

Figure 5. Simulation result for wood deposition patterns. Flow direction from bottom to top. Colour scale shows water depth (in metres). This figure is available in colour online at wileyonlinelibrary.com/journal/espl

According to the previous data available for this event, Scenario 2 seems to be the best in reproducing the bridge clogging and backwater elevation. For this scenario, the wood deposits are compared with post-event pictures (Figure 12). Figure 12 shows an agreement between the predicted depositional areas for SC2 and the observed deposits. According to the observed depositional areas for wood, most of the wood was deposited in the bridge section (this is well reproduced by the three scenarios, as can be observed in maps and graphs). Some pieces are deposited upstream from the bridge on both the left and right banks (between sections D and B); however, these deposits are not well predicted for SC3 (see Figure 5), where the right bank has a lack of wood, and in SC1 deposits are fewer on the left bank. Between sections A and B the pattern is generally well predicted for the three scenarios, with almost no deposits on the right bank, although a few pieces were found close to section B (this is well reproduced in SC2 and SC3). There is not much more information about wood deposits downstream from the bridge, but several pieces were observed on the right bank and only a few on the left bank. This is generally well predicted for Scenarios 2 and 3.

These patterns are related to hydrodynamics and riverbed morphology. As might be expected, wood is deposited in shallower flow regions and wood jams tend to be formed at lower flow velocities (Lyn *et al.*, 2007).

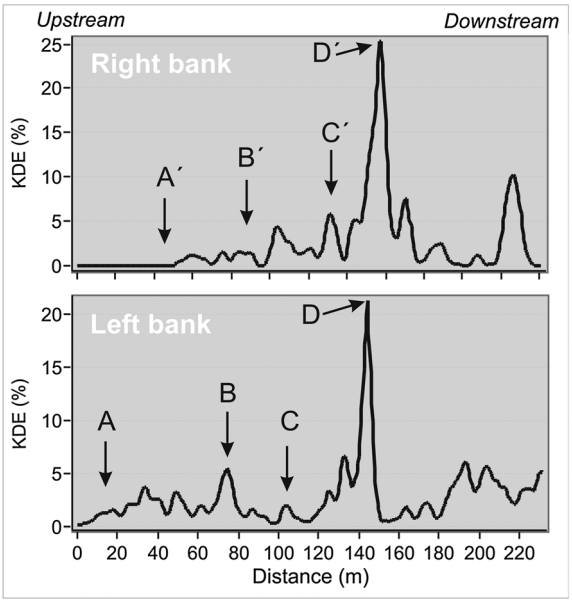

Figure 6. Average kernel density estimation (KDE, %) along the two banks for the three scenarios. Sections shown in Figure 5 are marked with arrows.

Discussion

A bridge clogging process due to LWM transport during a flash flood event was reproduced by modelling individual wood pieces moving in the flow, using a 2D hydrodynamic model with a new module to simulate wood transport.

Althought in general terms the results showed good agreements between field observations and modelling, some limitations should be highlighted. The main simplification assumed by the model is the shape of the logs as cylinders, disregarding the effect of branches or roots. This geometry is not representative of large wood with complex shapes (Allen and Smith, 2012) but can be a good approximation for key-pieces or non-rooted and defoliated trees (Braudrick *et al.*, 1997; Bocchiola *et al.*, 2008; Buxton, 2010; Mazzorana *et al.*, 2011), although, according to the findings of Schmocker and Hager (2010), the probability of blocking may increase with the presence of roots, in the case of conifers, for example. If branches or roots are present on the logs then the model can underestimate the blockage process, or may fail with regard to the log movement simulation. Braudrick and Grant (2000) proposed a theoretical method to attach the rootwad to a log using a disk on the cylinder ends. The authors expect to overcome this limitation in future developments.

The other important assumption here was estimation of the input wood volumes (Vw). Since there was neither evidence from eyewitnesses nor direct observations reporting what happened (regarding wood) during the 1997 flood, the methodology proposed by Ruiz-Villanueva *et al.* (2012b) was used to estimate the wood input rate. We first delineated the area affected by the flood and avulsion process based on previous work and field observations. This is an important issue, and could be a source of uncertainty if this area is unknown, or if simulating future or design scenarios and not past events. The methodology incorporates so-called vegetation resistance and the severity of the recruitment process. Vegetation resistance was established based on the tree species and stage of the forest, and on previous studies by Hutte (1968), Stumbles

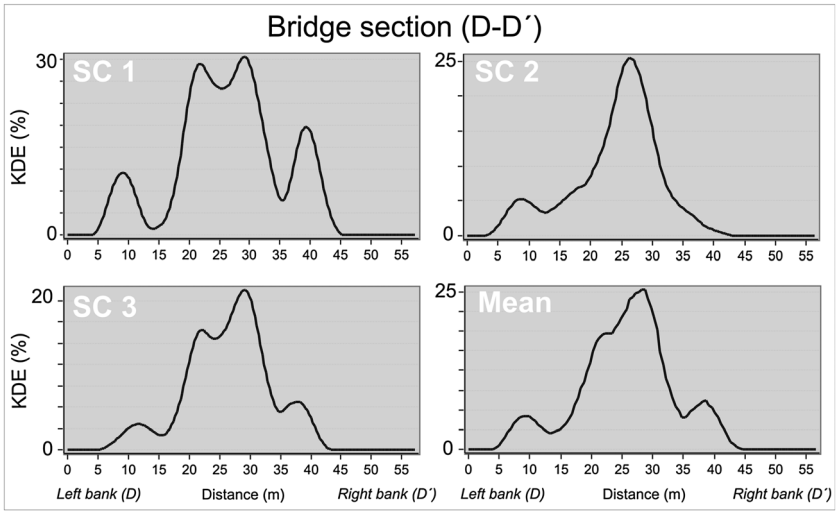

Figure 7. Kernel density estimation (KDE, %) for the bridge cross-section for each scenario and average.

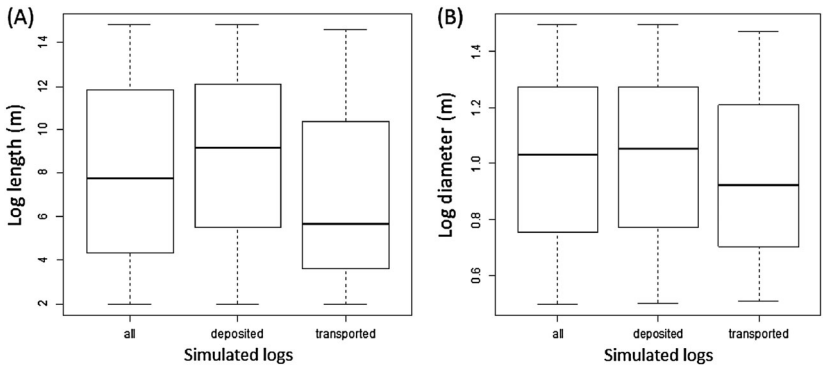

Figure 8. Boxplots of simulated logs, longitude (A) and diameter (B) values for SC2.

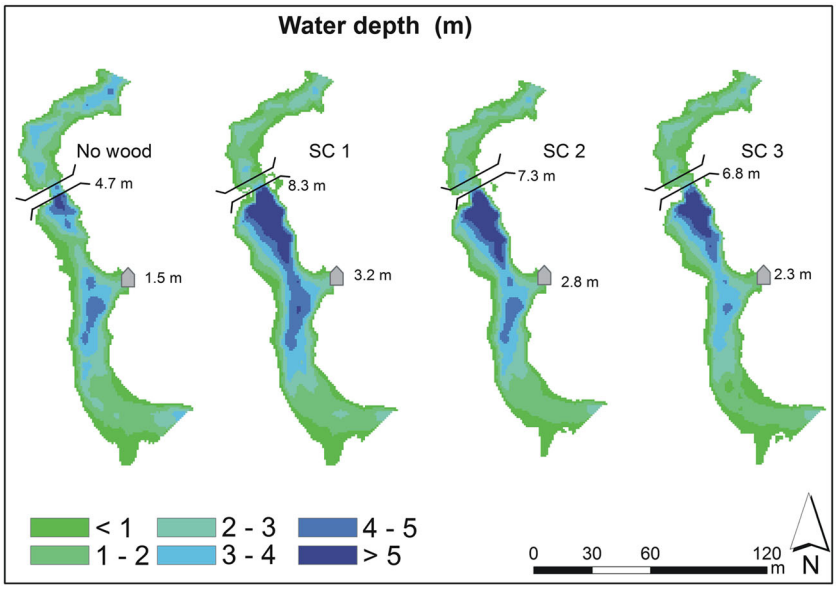

Figure 9. Water depth for the simulated hydrograph without wood, and for the three scenarios (SC1, SC2, and SC3). The black line represents the bridge, and the grey polygon the small white building (see Figure 1). Flow direction from bottom to top. This figure is available in colour online at wileyonlinelibrary.com/journal/espl

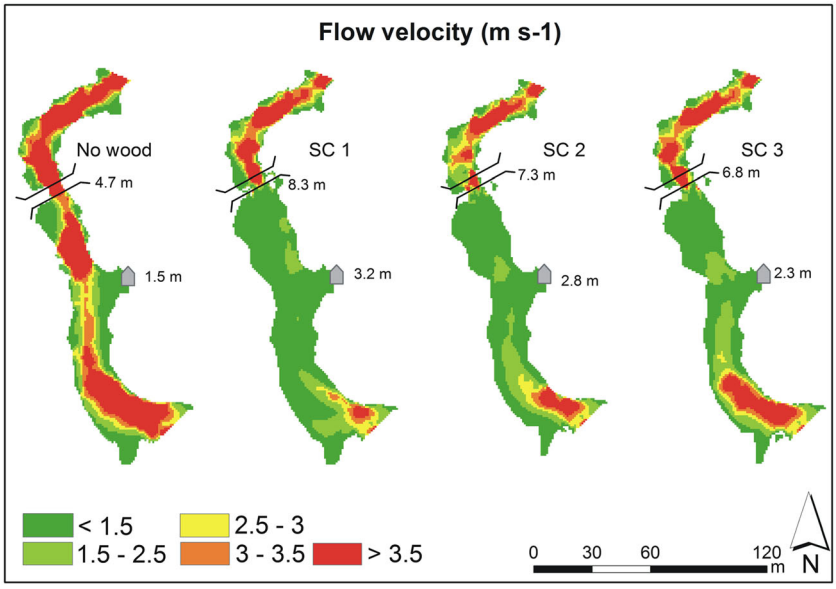

Figure 10. Flow velocity for the simulated hydrograph without wood, and for the three scenarios (SC1, SC2, and SC3). The black line represents the bridge, and the grey polygon the small white building (see Figure 1). Flow direction from bottom to top. This figure is available in colour online at wileyonlinelibrary.com/journal/espl

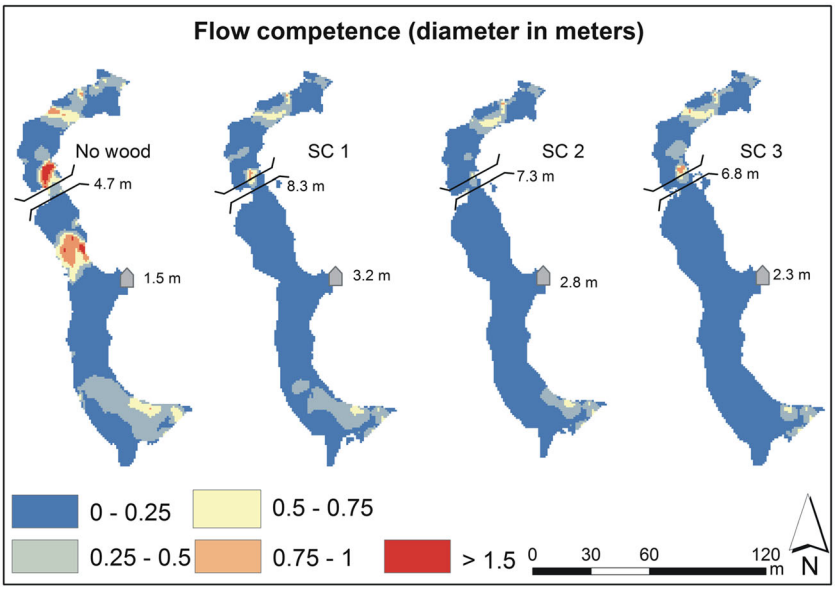

Figure 11. Flow competence (based on Shields shear, indicates the maximum boulder size the flow will be able to transport) for the simulated hydrograph without wood, and for the three scenarios (SC1, SC2, and SC3). The black line represents the bridge, and the grey polygon the small white building (see Figure 1). Flow direction from bottom to top. This figure is available in colour online at wileyonlinelibrary.com/journal/espl

Table III. Summary of simulations for the four scenarios (no wood, and three scenarios of wood transport): water depth at the bridge section; water depth at the small white building, mean flow velocity for the studied reach (SD, standard deviation), number of logs deposited and percentage of the bridge obstruction

Scenario	Water level at SB (m)	Water level at SWB (m)	Mean (SD) flow velocity (m s^{-1})	Deposited wood	Percent bridge obstruction
No wood	4·7	1·5	3·00 (1·88)	—	—
SC1	8·3	3·2	1·45 (1·35)	213	> 70
SC2	7·3	2·8	1·63 (1·28)	180	~50
SC3	6·8	2·3	1·94 (1·40)	137	< 40
Previous estimates	7·1	2·9	3·5 (without obstruction), 1·25 (1·09)	—	48 ± 8

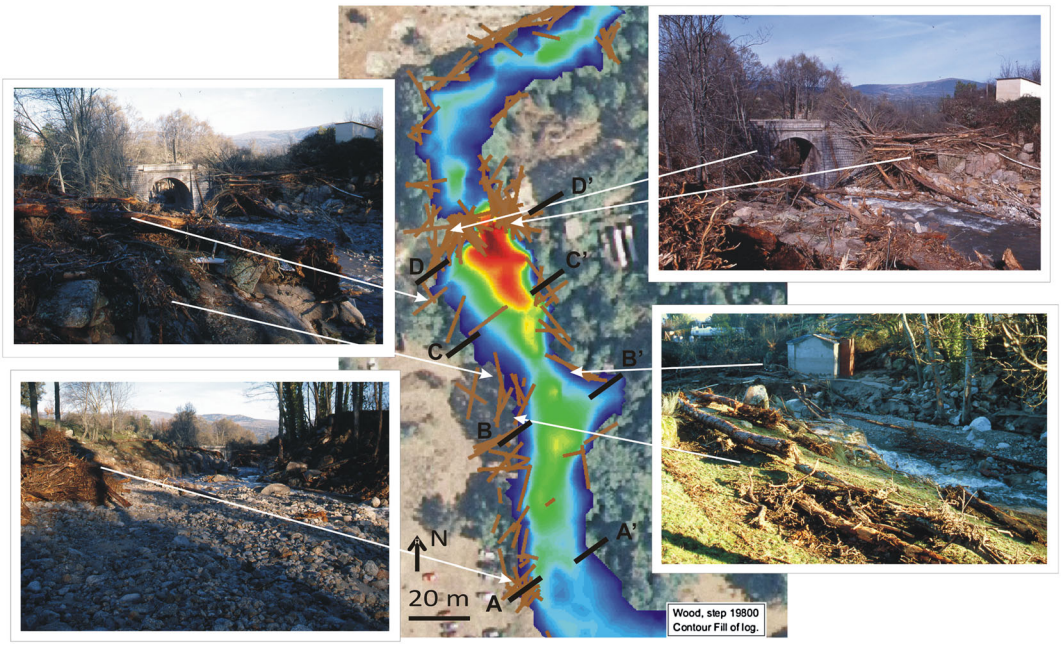

Figure 12. Field observations and simulation result for SC2. This figure is available in colour online at wileyonlinelibrary.com/journal/espl

(1968), Naka (1982) and Abernethy and Rutherfurd (2001). This concept may be equivalent to the structural classification of forested areas posited by Blaschke *et al.* (2004) and the large wood availability indicator used by Mazzorana *et al.* (2011). The volume correction factor can be a source of subjectivity, and modification of this coefficient could change the final results. The probability of a tree being recruited was quantified using the volume correction factor. This factor reduces the total volume

of potential recruitable wood in those areas where vegetation resistance is highest or recruitment process less intense. The resulting values cannot be validated but can be assumed as orders of magnitude and moreover a range was considered to take into account uncertainty.

The establishment of different scenarios for the wood transport allowed us to study the influence of the inlet boundary conditions on the wood clogging of the bridge and deposits patterns. These scenarios were established based on previous knowledge of the area and the event studied. As expected, steady transport (SC3) is associated with a lower probability of blocking, whereas congested transport (SC1) resulted in the highest blocking rate.

Scenario generation is a powerful tool that can be found in various different studies (Scholz and Tietje, 2002), and we have used it throughout this research, similar to other authors who also proposed it as an analytical approach for risk analysis in mountain areas (Mazzorana and Fuchs, 2010; Mazzorana *et al.*, 2010, 2011; Rigon *et al.*, 2012). The scenarios generated in this study were defined according to the proposals of Godet (1986) to identify the smallest number of possibilities that may represent various states, including the so-called worst-case scenario. In this case, SC3 may represent a steady transport usually observed during high flows; SC2 may represent the expected transport during a flash flood, where the flow transport capacity increases suddenly during the rising limb and is at its maximum before the peak, before decreasing more slowly during the recession limb; and finally SC1 may represent the worst-case scenario, like a sudden arrival of a large amount of wood, usually observed during dam breaks. The ultimate goal is to obtain different possibilities for evaluating likely or possible situations, in this paper related to the influence of woody material in the 1997 flood and related wood deposits.

Furthermore, sediment transport also took place during the studied episode, as can be observed in the pictures, and this could have a significant effect because it may also influence the bridge clogging process. However, this study has focused on the reconstruction and simulation of wood transport, so it would be advisable to carry out further analysis to better incorporate both wood and sediment transport processes.

Conclusions

This paper shows how the impact (in terms of water depth and flooded areas) of a flash flood may increase due to the transport of large quantities of wood, particularly at critical sections, such as bridges. Large wood transport should therefore not be discarded from flood analyses, at least in forested basins. However, the wide spatial and temporal variability associated with wood recruitment coupled with complex transport mechanics may make such analysis particularly challenging. The numerical model presented here represents a powerful tool for simulating the transport of wood together with hydrodynamics. This model is able to predict and simulate patterns of wood deposits, and reproduce the interaction between wood and infrastructures. The results of the 1997 event simulation showed the main depositional zones or areas prone to form wood jams and the probability of a log to be blocked in the bridge section. Moreover, the increase in water level and the change in flow velocity due to the bridge clogging were also reproduced by the model.

Applying this model to the case study highlights its viability, although as usual in modelling approaches, some simplifications are assumed. Field data and an in-depth knowledge of the riparian forest and in-stream wood must be obtained to establish inlet boundary conditions and appropriately validate results. Even if these empirical data are not available, it may still be used as an alternative and supplementary tool for generating scenarios.

Acknowledgements—The authors express their gratitude to the Spanish Ministry of Science and Innovation for the financial support received. This work was funded by the MAS Dendro-Avenidas project (CGL2010-19274) and the Geological Survey of Spain (IGME). The authors are grateful to the Tagus Water Authority, Environment Department of Castilla y León in Ávila, and Navaluenga Council for their collaboration. Special thanks to Ignacio Gutiérrez for his help with the topographical survey. Thanks to the contribution of Professor S. N. Lane, Dr Francesco Comiti and one anonymous reviewer, for strongly improving the quality of the earlier version of this manuscript.

References

Abernethy B, Rutherfurd ID. 2001. The distribution and strength of riparian tree roots in relation to riverbank reinforcement. *Hydrological Processes* **15**: 63–79.

Allen JB, Smith DL. 2012. Characterizing the impact of geometric simplification on large woody debris using CFD. *International Journal of Hydraulic Engineering* **1**: 1–14.

Ballesteros JA, Bodoque JM, Díez-Herrero A, Sanchez-Silva M, Stoffel M. 2011a. Calibration of floodplain roughness and estimation of palaeoflood discharge based on tree-ring evidence and hydraulic modelling. *Journal of Hydrology* **403**: 103–115.

Ballesteros JA, Eguiba M, Bodoque JM, Díez-Herrero A, Stoffel M, Gutiérrez-Pérez I. 2011b. Estimating flash flood discharge in an ungauged mountain catchment with 2D hydraulic models and dendrogeomorphic paleostage indicators. *Hydrological Processes* **25**: 970–979.

Benda LE, Sias JC. 2003. A quantitative framework for evaluating the mass balance of in-stream organic debris. *Forest Ecology and Management* **172**: 1–16.

Benda L, Miller D, Sias J, Martin D, Bilby R, Veldhuisen C, Dunne T. 2003. Wood recruitment processes and wood budgeting. *Ecology and Management of Wood in World Rivers* **37**: 49–73.

Bladé E, Cea L, Corestein G, Escolano E, Puertas J, Vázquez-Cendón ME, Dolz J, Coll, A. 2012a. Iber – Herramienta de simulación numérica del flujo en ríos. *Revista Internacional de Métodos Numéricos para Cálculo y Diseño en Ingeniería*. http://www.sciencedirect.com/science/article/pii/S0213131512000454

Bladé E, Gómez-Valentín MJ, Aragón-Hernández D, Corestein G, Sánchez-Juny M. 2012b. Integration of 1D and 2D finite volume schemes for computations of water flow in natural channels. *Advances in Water Resources* **42**: 17–29.

Blaschke T, Tiede D, Heurich M. 2004. 3D landscape metrics to modelling forest structure and diversity based on Laser scanning data. *The International Archives of Photogrammetry, Remote Sensing and Spatial Information Sciences*, vol. XXXVI-8/W2. International Archives of Photogrammetry: Freiburg; 129–132.

Bocchiola D, Catalano F, Menduni G, Passoni G. 2002. An analytical–numerical approach to the hydraulics of floating debris in river channels. *Journal of Hydrology* **269**: 65–78. DOI: 10.1016/S0022-1694(02)00195-6

Bocchiola D, Rulli M, Rosso R. 2006 Transport of large woody debris in the presence of obstacles. *Geomorphology* **76**: 166–178.

Bocchiola D, Rulli MC, Rosso R. 2008. A flume experiment on the formation of wood jams in rivers. *Water Resources* **44**: 1–17.

Bodoque JM, Eguibar MA, Díez-Herrero A, Gutiérrez-Pérez I, Ruiz-Villanueva V. 2011. Can the discharge of a past hyperconcentrated flow be estimated based on palaeoflood evidence? *Water Resources Research* W12535. DOI: 10.1029/2011WR010380

Bragg DC, Kershner L. 2004. Sensitivity of a riparian large woody debris recruitment model to the number of contributing banks and tree fall pattern. *Western Journal of Applied Forestry* **19**: 117–122.

Braudrick C, Grant GE. 2000. When do logs move in rivers? *Water Resources Research* **36**: 571.

Braudrick CA, Grant GE, Ishikawa Y, Ikeda H. 1997. Dynamics of wood transport in streams: a flume experiment. *Earth Surface Processes and Landforms* **22**: 7.

Braudrick CA, Grant GE, Northwest P, Forest US. 2001. Transport and deposition of large woody debris in streams: a flume experiment. *Geomorphology* **41**: 263–283.

Brooks AP, Abbe T, Cohen T, Marsh N, Mika S, Boulton A, Broderick T, Borg D, Rutherfurd I. 2006. Design guidelines for the reintroduction of wood into Australian streams. Land & Water: Australia, Canberra.

Buxton TH. 2010. Modeling entrainment of waterlogged large wood in stream channels. *Water Resources Research* **46**: DOI: 10.1029/2009WR008041

Carlson J, Andrus C, Froelich H. 1990. Woody debris, channel features, and macroinvertebrates of streams with logged and undisturbed riparian timber in northeastern Oregon, U.S.A. *Canadian Journal of Fisheries and Aquatic Sciences* **47**: 1103–1111.

Comiti F, Andreoli A, Mao L, Lenzi MA. 2008. Wood storage in three mountain streams of the southern Andes and its hydro-morphological effects. *Earth Surface Processes and Landform* **33**: 244–262.

Comiti F, Agostino VD, Moser M, Lenzi MA, Bettella F, Agnese AD, Rigon E, Gius S, Mazzorana B. 2012. Preventing wood-related hazards in mountain basins: from wood load estimation to designing retention structures. *Proceedings, 12th Congress INTERPRAEVENT 2012*, Grenoble, France; 651–662.

Corestein G, Bladé E, Cea L, Lara Á, Escolano E. 2010. Iber, a river dynamics simulation tool A: Conference on Advances and Applications of GiD. "GiD 2010 - 5th Conference on Advances and Applications of GiD". Barcelona: Centro Internacional de Métodos Numéricos en Ingeniería (CIMNE), 2010, p. 47–50.

Diehl TH. 1997. Potential Drift Accumulation at Bridges. Publication No. FHWA-RD-97-028. US Department of Transportation, Federal Highway Administration Research and Development, Turner-Fairbank Highway Research Center: McLean, VA. http://www.tn.water.usgs.gov/pubs/FHWA-RD-97-028/drfront1.htm

Díez-Herrero A. 2003. Geomorfología e Hidrología fluvial del río Alberche. Modelos y SIG para la gestión de riberas. Serie Tesis Doctorales. Publicaciones del Instituto Geológico y Minero de España (Ministerio de Ciencia y Tecnología): Madrid; 587.

Dudley SJ, Fischenich JC, Abt SR. 1998. Effect of woody debris entrapment on flow resistance. *Journal of the American Water Resources Association* **34**: 1189–1197. DOI: 10.1111/j.1752-1688.1998.tb04164.x

Fischer M. 2006. Driftwood During the Flooding in Klosters in 2005, Report, HSW Wädenswil, Switzerland (in German). http://www.wsl.ch/fe/walddynamik/projekte/schwemmholzablagerungen/index_EN

Gippel CJ. 1995. Environmental hydraulics of large woody debris in streams and rivers. *Journal of Environmental Engineering* **121**: 388.

Gippel CJ, White K. 2000. Re-introduction techniques for instream large woody debris. In A Rehabilitation Manual for Australian Streams, Volume **1**, Rutherfurd ID, Jerie K, Marsh N (eds). Land and Water Resources Research and Development Corporation and Cooperative Research Centre for Catchment Hydrology: Canberra; 313–321.

Godet M. 1986. Introduction to 'la prospective': seven key ideas and one scenario method. *Futures* **2**(2): 134–157.

Gregory S, Boyer KL, Gurnell AM. 2003. The ecology and management of wood in world rivers. *American Fisheries Society Symposium* **37**: 431

Gurnell AM, Piegay H, Swanson FJ, Gregory SV. 2002. Large wood and fluvial processes. *Freshwater Biology* **47**: 601–619.

Haga H. 2002. Transport and retention of coarse woody debris in mountain streams: an in situ field experiment of log transport and a field survey of coarse woody debris distribution. *Water Resources Research* **38**(8): 1-1–1-16.

Hutte P. 1968. Experiments on windflow and wind damage in Germany: site and susceptibility of spruce forests to storm damage. *Forestry* **41**: 20–26.

Jackson CR, Sturm CA. 2002. Woody debris and channel morphology in first- and second-order forested channels in Washington's coast ranges. *Water Resources Research* **38**: 1177–1190.

Langford TEL, Langford J, Hawkins SJ. 2012. Conflicting effects of woody debris on stream fish populations: implications for management. *Freshwater Biology* **57**(5): 1096–1111. DOI: 10.1111/j.1365-2427.2012.02766.x

Lassettre NS, Harris RR. 2001. The Geomorphic and Ecological Influence of Large Woody Debris in Streams and Rivers. University of California: Berkeley, CA; 68.

Lassettre NS, Kondolf GM. 2012. Large woody debris in urban stream channels: redefining the problem. *River Research and Applications* **28**(9): 1477–1487. DOI: 10.1002/rra

Lyn D, Cooper T, Condon D, Gan L. 2007. Factors in Debris Accumulation at Bridge Piers, Washington. US Department of Transportation, Federal Highway Administration Research and Development, Turner-Fairbank Highway Research Center: McLean, VA.

MacVicar BJ, Hervé P, Henderson A, Comiti F, Oberlin C, Pecorari E. 2009. Quantifying the temporal dynamics of wood in large rivers: field trials of wood surveying, dating, tracking, and monitoring techniques. *Earth Surface Processes and Landforms* **34**: 2031–2046.

Manga M, Kirchner JW. 2000. Stress partitioning in streams by large woody debris. *Water Resources* **36**: 2373–2379.

Mao L, Burns S, Comiti F, Andreoli A, Urciolo A, Gavino-Novillo M, Iturraspe R, Lenzi MA. 2008. Acumulaciones de detritos leñosos en un cauce de Montaña de Tierra del Fuego: Análisis de la movilidad y de los efectos hidromorfologicos. *Bosque* **29**: 197–211.

Martin DJ, Benda LE. 2001. Patterns of instream wood recruitment and transport at the watershed scale. *Transactions of the American Fisheries Society* **130**: 940–958.

May CL, Gresswell RE. 2003. Large wood recruitment and redistribution in headwater streams in the southern Oregon Coast Range, U.S.A. *Canadian Journal of Forest Research* **33**: 1352.

Mazzorana B, Fuchs S. 2010. Fuzzy formative scenario analysis for woody material transport related risks in mountain torrents. *Environmental Modelling & Software* **25**: 1208–1224.

Mazzorana B, Zischg A, Largiader A, Hübl J. 2009. Hazard index maps for woody material recruitment and transport in alpine catchments. *Natural Hazards and Earth System Science* **9**: 197–209.

Mazzorana B, Hübl J, Zischg AM, Largiader A. 2010. Modelling woody material transport and deposition in alpine rivers. *Natural Hazards* **56**(2): 425–449.

Mazzorana B, Comiti F, Volcan C, Scherer C. 2011. Determining flood hazard patterns through a combined stochastic–deterministic approach. *Natural Hazards* **59**(1): 301–316.

Merten E, Finlay J, Johnson L, Newman R, Stefan H, Vondracek B. 2010. Factors influencing wood mobilization in streams. *Water Resources Research* **46**: 1–13.

MFE. 2011. El Mapa Forestal de España 1:25000 (MFE). Ministerio de Agricultura, Alimentación y Medio Ambiente (MARM). http://www.magrama.es/es/biodiversidad/temas/montes-y-politica-forestal/mapa-forestal/mfe_25.aspx

Montgomery D. 2003. Wood in rivers: interactions with channel morphology and processes. *Geomorphology* **51**: 1–5.

Naka K. 1982. Community dynamics of evergreen broadleaf forests in southwestern Japan. I. Wind damaged trees and canopy gaps in an evergreen oak forest. *Journal of Plant Research* **95**: 385–399.

Nakamura F, Swanson FJ, Wondzell SM. 2000. Disturbance regimes of stream and riparian systems? A disturbance-cascade perspective. *Hydrological Processes* **14**: 2849–2860.

Palacios D, Marcos J, Vázquez-Selem L. 2010. Last glacial maximum and deglaciation of Sierra de Gredos, Central Iberian Peninsula. *Quaternary Internacional* **233**: 16–26.

Rigon E, Comiti F, Lenzi M. 2012. Large wood storage in streams of the eastern Italian Alps and the relevance of hillslope processes. *Water Resources Research* **48**. DOI: 10.1029/2010WR009854

Robison EG, Beschta RL. 1990. Characteristics of coarse woody debris for several coastal streams of southeast Alaska: USA, *Can. J. Fish. Aquat. Sci* **47**: 1684–1693.

Rosso R, Rulli MC, Bocchiola D. 2007. Transient catchments hydrology after wildfires in a Mediterranean watershed: runoff, sediment and woody debris. *Hydrology and Earth System Sciences* **11**: 125–140.

Ruiz-Villanueva V. 2012. *Nuevas metodologías en la evaluación de la peligrosidad y el riesgo por avenidas en cuencas de montaña* [*New*

methods for the analysis of flash flood hazard and risk in Mountain basins]. PhD Thesis. Universidad Complutense de Madrid (unpublished). http://cisne.sim.ucm.es/search~S2*spi?/hT+1414/hT!x+!d1414/-3%2C-1%2C0%2CB/frameset&FF=hT!x+!d1414&2%2C%2C2

Ruiz-Villanueva V, Bodoque JM, Díez-Herrero A, Calvo C. 2011. Triggering threshold precipitation and soil hydrological characteristics of shallow landslides in granitic landscapes. *Geomorphology* **133**: 178–189.

Ruiz-Villanueva V, Bodoque JM, Díez-Herrero A, Eguibar MA, Pardo-Igúzquiza E. 2012a. Reconstruction of an ungauged flash flood event with large wood transport and its influence on hazard patterns. *Hydrological Processes*. DOI: 10.1002/hyp.9433

Ruiz-Villanueva V, Díez-Herrero A, Ballesteros JA, Bodoque JM. 2012b. Potential large woody debris recruitment due to landslides, bank erosion and floods in mountain basins: a quantitative estimation approach. *River Research and Applications*. DOI: 10.1002/rra.2614

Ruiz-Villanueva V, Bladé-Castellet E, Sánchez-Juny M, Martí B, Díez Herrero A, Bodoque JM. Submitted for publication. Two dimensional numerical modelling of wood transport. *Journal of Hydroinformatics*.

Schmocker L, Hager WH. 2010. Drift accumulation at river bridges. In River Flow, Dittrich A, Koll Ka, Aberle J, Geisenhainer P (eds). Bundesanstalt für Wasserbau: Karlsruhe.

Schmocker L, Hager WH. 2011. Probability of drift blockage at bridge decks. *Journal of Hydraulic Engineering* **137**: 480–492.

Scholz RW, Tietje O. 2002. Embedded Case Study Methods: Integrating Quantitative and Qualitative Knowledge. Sage Publications: London.

Seo JI, Nakamura F, Nakano D, Ichiyanagi H, Chin KW. 2008. Factors controlling the fluvial export of large woody debris, and its contribution to organic carbon budgets at watershed scales. *Water Resources Research* **44**: DOI: 10.1029/2007WR006453

Stumbles RE. 1968. How wind influences silviculture and management as a district officer sees it. *Forestry* Supplement: 45–50.

Swanson FJ. 2003. Wood in rivers: a landscape perspective. *American Fisheries Society Symposium* **37**: 299–313.

Waldner P, Rickli C, Köchlin D, Usbeck T, Schmocker L, Sutter F. 2007. Schwemmholz. Ereignisanalyse Hochwasser 2005 – Teil 1: Prozes se, Schäden und erste Einordnung (in German). Bundesamt für Umwelt BAFU, Eidgenössische Fors chungsanstalt WSL. Bezzola GR, Hegg C (eds). *Umwelt-Wissen* **0825**: 181–193.

Welty JJ, Beechie T, Sullivan K, Hyink DM, Bilby RE, Andrus C, Pess G. 2002. Riparian aquatic interaction simulator (RAIS): a model of riparian forest dynamics for the generation of large woody debris and shade. *Forest Ecology and Management* **162**: 299–318.

Young WJ. 1991. Flume study of the hydraulic effects of la rge woody debris in lowland rivers. *Regulated Rivers: Research & Management* **6**: 203–212.